Measurement of analyzing powers of the ^{1}H(d,^{3}He)γ reaction at 17.5 MeV

H. Akiyoshi,* K. Sagara, S. Ueno, N. Nishimori,† T. Fujita, K. Maeda, H. Nakamura,‡ and T. Nakashima
Department of Physics, Kyushu University, Fukuoka 812-8581, Japan
(Received 19 July 2000; revised manuscript received 9 March 2001; published 6 August 2001)

Analyzing powers $A_{xx}(\theta)$, $A_{yy}(\theta)$, $A_{zz}(\theta)$, and $A_y^d(\theta)$ of the H($\vec{d}$,^{3}He)γ reaction were measured at $E_d = 17.5$ MeV. A hydrogen gas target sealed with thin carbon foils was used and the angular distribution of ^{3}He recoils was observed to measure the analyzing powers. High-statistics data were obtained over a wide c.m. angular range. The results are compared with recent Faddeev calculations based on the realistic two body potential with and without three-nucleon force incorporated.

DOI: 10.1103/PhysRevC.64.034001 PACS number(s): 25.10.+s, 24.70.+s, 25.40.Lw

I. INTRODUCTION

It is well known that the binding energies of three-nucleon systems are underpredicted by the calculation with realistic two-nucleon forces ($2NF$). The problem has been demonstrated to be solved by incorporating three-nucleon force [1], which is considered to originate from two pion exchange among three nucleons ($\pi\pi 3NF$). Although use of an adjustable parameter for πNN coupling strength in the calculation still needs a justification, the correct prediction of the binding energies appears to indicate the existence of the $\pi\pi 3NF$.

Another possible evidence for $3NF$ may be seen in the differential cross section of the pd scattering. At the minimum of angular distribution of the cross section, a systematic deviation of the calculation from the observed cross section has first been reported in the energy region of $E_p = 2-18$ MeV [2]. Koike and Ishikawa [3] have later pointed out that the discrepancy also exists at higher energies. Witała *et al.* [4] have shown that the discrepancy is successfully reduced at higher energies ($E_p \geqslant 65$ MeV) by introducing the $\pi\pi 3NF$ with the same parameter as used in the binding energy calculation for the $3N$ systems. These facts together seem to claim the existence of the $\pi\pi 3NF$ and further evidence are definitely desired to confirm the possible contribution of $3NF$ in the $3N$ systems.

On the other hand, there have been reports of such discrepancies between experiment and calculation that are not explained by $\pi\pi 3NF$. Discrepancies of $20-30\%$ still remain in the analyzing power A_y of the Nd scattering below 30 MeV [5] (often referred to as the A_y puzzle), and $10-20\%$ differences exist in the Nd breakup cross section in the space star configuration at around 13 MeV [6–8]. The recent Faddeev calculation, which has taken into account Coulomb force, has also claimed an existence of $5-10\%$ discrepancies in the pd scattering cross section at around 10 MeV [9]. Reproducibility of the calculation seems to be especially poor for A_{xx} and A_{yy} of the pd breakup reaction in some kinematical condition at $E_d = 52$ MeV [10]. All these are not solved by introducing the $\pi\pi 3NF$ and suggest that some imperfection still remains in the realistic $2NF$. Study of $3NF$, therefore, requires further examinations on new kinds of three body observables with careful discrimination of the inadequacy of $2NF$.

In the present paper, we report the measurement of analyzing powers of the $p+d \rightarrow {}^3\mathrm{He}+\gamma$ reaction at $E_d = 17.5$ MeV. The aim is to see the possible effect of $3NF$ in the analyzing powers of the pd radiative capture reaction which may reflect the effects of the $\pi\pi 3NF$ in the $3N$ bound state. For this kind of reaction, Ishikawa and Sasakawa [11] have suggested from their nd capture calculation that the $\pi\pi 3NF$ effect is less than 10% in A_{yy} at $E_d = 10-30$ MeV. This would indicate that the experimental accuracy should be less than a few percent to look for a signature of $3NF$. It is also to be noted that the calculation to be compared with the experiment should be performed accurately by including not only the dominant $E1$ transition but also minor contributions of the $M1$ and $E2$ components.

The cross section of the pd radiative capture is very small ($\leqslant 1.5$ μb/sr), which makes the experimental observation rather difficult. In the case of the detection of γ rays from the reaction, very thick ($21-35$ mg/cm^2) liquid hydrogen targets have been used at rather high beam energy of above 29 MeV to obtain high-statistics data [12,13]. A high experimental efficiency is expected in the detection of ^{3}He recoils rather than in the detection of γ rays. It may be worth notice that the ^{3}He recoils are emitted in a narrow forward cone centered at zero degree. A drawback, however, is in the requirement that the target should be thin enough to reduce the angular and energy spreads of the ^{3}He recoils. In the previous works which have adopted the ^{3}He detection [14,15], polyethylene foil targets have been used and the carbon contents have limited the hydrogen thicknesses of the targets. The poor mechanical strength of polyethylene against the beam bombardment has also been an important disadvantage.

In the present work, a thick hydrogen gas target was specially developed to allow a precise measurement of ^{3}He recoils at $E_d = 17.5$ MeV. The new target was as thick as

*Present address: Cyclotron Center, RIKEN, 2-1 Hirosawa, Wako, Saitama 351-0198, Japan.
†Present address: FEL Laboratory, Japan Atomic Energy Research Institute, Tokai, Naka, Ibaragi 319-1195, Japan.
‡Present address: Kitakyushu National College of Technology, Shii, Kokura-Minami-Ku, Kitakyushu, Fukuoka 802-0985, Japan.

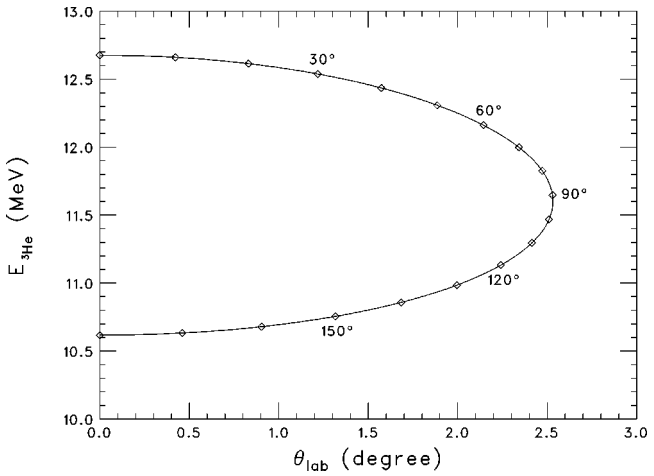

FIG. 1. Energy vs lab angle of ^{3}He from H$(d,^3\mathrm{He})\gamma$ reaction at $E_d=17.5$ MeV, plotted at every 10° of c.m. angle.

0.13 mg/cm^2 and was found to stand the beam of an intensity as high as 1 μA, making a high-statistics measurement feasible in the angular distributions of $A_{xx}(\theta)$, $A_{yy}(\theta)$, $A_{zz}(\theta)$, and $A_y^d(\theta)$ of the pd radiative capture reaction in a wide c.m. angular range.

II. EXPERIMENTAL PROCEDURE

In the $p+\vec{d}\rightarrow{}^3\mathrm{He}+\gamma$ reaction with deuteron beam of 17.5 MeV, ^{3}He particles are emitted at forward laboratory angles within 2.6° with energies shown in Fig. 1. The measurement of the angle and energy of the ^{3}He recoils at these forward angles enables, in principle, the observation of events in the whole angular range of γ-ray emission.

The setup for the H$(\vec{d},^3\mathrm{He})\gamma$ experiment is schematically shown in Fig. 2. A 90° deflecting dipole magnet, placed downstream from the H_2 target, separates the ^{3}He recoils from the incident $\vec{d}$ beam. The $\vec{d}$ beam was stopped on a Faraday cup located in the gap of the magnet and the ^{3}He recoils were detected by a large Si detector of 60 mm $\times$60 mm in area placed behind the magnet. Since the incident beam was observed to accompany a large number of low-energy deuterons (beam halo), a 4° deflecting magnet was placed in the beam line to prevent such contaminations from hitting the target. The use of the magnet reduced the number of low-energy deuterons reaching the detector by two orders of magnitude.

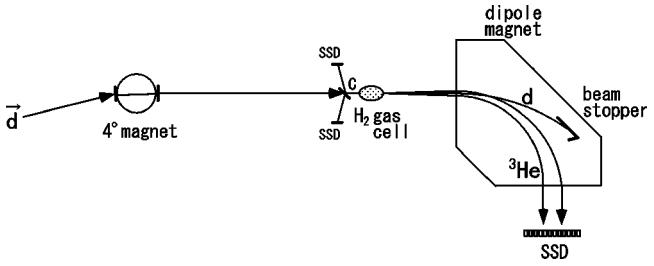

FIG. 2. Schematic layout of the experimental setup for H$(\vec{d},^3\mathrm{He})\gamma$ reaction. The $\vec{d}$-beam polarization was monitored in front of the gas target using $^{12}\mathrm{C}+\vec{d}$ scattering.

A. Gas target

As mentioned above, a hydrogen gas target was used to minimize the angular and energy spreads of the ^{3}He recoils and to achieve a high mechanical stability against the beam bombardment. The target used was 0.5 atm hydrogen gas contained in a cell of 3 cm in length ($=0.13$ mg/cm^2) along the beam direction. The windows of the cell were of 5 mm in diameter at the entrance and of 5 mm$\times$10 mm in area at the exit. Window foils were glued to the inner cell walls, which were curved with a 6 mm radius of curvature, so that the gas pressure may not cause too large a mechanical tension in the window foils.

Carbon foils of 0.36 mg/cm^2 in thickness were used for the window foils. Since ^{12}C and ^{13}C have large negative Q values for $(d,^3\mathrm{He})$ reactions, carbon is the best suited material in eliminating ambiguities to be caused by the ^{3}He particles produced in the window foils. In order to increase the mechanical strength of the carbon foil, a special procedure was adopted for fabrication. Carbon was vacuum evaporated onto a glass plate by the arc-discharge method. The discharge was repeated approximately 6000 times at intervals of approximately 12 s with occasional pauses to cool the glass backing. The maximum gas pressure that can be supported by the foil was measured to be 1.2 and 0.7 atm, respectively, at the entrance and the exit window of the target cell.

In the present experiment, the target gas pressure was kept at 0.5 atm. The energy and angular spreads of ^{3}He recoils caused by the target were estimated to be, respectively, 120 keV and 0.31°, which are to be compared with 350 keV and 0.43°, estimated for a polyethylene target of an equivalent hydrogen thickness.

B. Polarized beam

A polarized d beam was produced in a Lamb-shift type ion source at the Kyushu university tandem accelerator facility. After the beam was accelerated to 30 keV, the polarization axis was rotated by a Wien filter into the beam (z) direction, the vertical (y) direction, and the side (x) direction for the measurement of A_{zz}, A_{yy} (and A_y^d), and A_{xx}, respectively. The magnetic substate of the polarized deuteron was cyclically changed over $m_z=1$, 0, and -1 states and kept for 10, 20, and 10 s, respectively. This was made by changing the magnetic field strength of the Lamb-shift ion source and each change took about 0.1 s. The data acquisition was paused for 1 s after each change to avoid the effect of possible instabilities of the ion source.

The tensor polarization of the $\vec{d}$ beam was monitored by using $^{12}\mathrm{C}+\vec{d}$ elastic scattering, for which A_{xx}, A_{yy}, and A_{zz} have high local maxima at 102°, 105°, and 107°, respectively. For this purpose, a carbon foil of 0.5 mg/cm^2 in thickness was placed just upstream the hydrogen target and

two Si detectors were placed to the left and the right of the beam symmetrically at the angles of the local maxima, depending on the beam polarization to form a polarimeter (see Fig. 2). The monitoring was continuously made throughout the experiment.

The magnetic substates of $m_z=1$, 0, and -1 have the tensor polarizations of $p_{zz}=1$, -2, and 1, and the vector polarizations of $p_z=1$, 0, and -1, respectively. Using the relation between p_{zz} and p_z and taking into accounts the slight depolarization caused by the finite size of the beam in the Lamb-shift ion source, the vector polarization of the beam was estimated from the measured tensor polarization.

The values of A_{xx}, A_{yy}, and A_{zz} of the $^{12}C+\vec{d}$ scattering at around 105° were determined in a separate experiment to the accuracy of 2%. In this experiment, the tensor polarization of the $\vec{d}$ beam was determined by a $^3He(\vec{d},p)$ polarimeter, the $A_{zz}(0°)$ of which had already been calibrated in our laboratory within an accuracy of 1% using the theoretical analyzing power of $^{16}O(\vec{d},\alpha_3)$ reaction.

C. Detection of ^{3}He

The ^{3}He recoils were detected by a Si strip detector of 60 mm $\times$60 mm in area, with 12 strips each of 4.89 mm in width, arranged at a spacing of 0.11 mm. The detector was so set as to place the strips vertically. To define the azimuthal angles of the measurement, a vertical slit of 12 mm in width was placed in front of the detector. From the simulation using an optics computer code ORBIT [16], the angular range defined by the slit was estimated to be $\pm 0.43°$ for the ^{3}He recoils in the laboratory frame at the target.

Position spread of ^{3}He particles on the detector was caused by multiple scattering in the target and the energy spread due to the finite thickness of the target. The overall position spread was estimated from the simulation to be 4.3 and 4.5 mm in the vertical and horizontal directions, respectively.

Since the ^{3}He events form an ellipselike curve in the plot of ^{3}He energy versus incidence position on the detector, the energy spectrum from each detector strip usually consists of two peaks corresponding to different reaction angles as seen in Fig. 3. The low- and high-energy peaks labeled ^{3}He in the spectrum correspond to the ^{3}He recoils ejected to the left- and the right-hand sides of the beam axis, respectively. The background spectra were obtained by evacuating the target gas and an example for the case of Fig. 3 is also shown by a dashed line in the figure. Although the detailed structures of the background spectra were not explored any further, the subtraction was successfully made without ambiguity.

D. Data analysis

The energy spectrum for each detector strip was well explained by the computer simulation and hence the reaction angles $\theta_{lab}(^3He)$ were estimated from the simulation in the practical data analysis. The angular ranges covered by the detector were $67° \leqslant \theta_{c.m.}(^3He) \leqslant 156°$ at the left-hand side and $18° \leqslant \theta_{c.m.}(^3He) \leqslant 115°$ at the right-hand side. From the width of the detector strip as well as the angular spreads of the ^{3}He recoils as given in the previous subsection, the experimental resolution of $\theta_{c.m.}(^3He)$ was estimated to be 8.4°, 6.0° (minimum), and 7.4° at $\theta_{c.m.}(^3He)=23°$, 115°, and 151°, respectively.

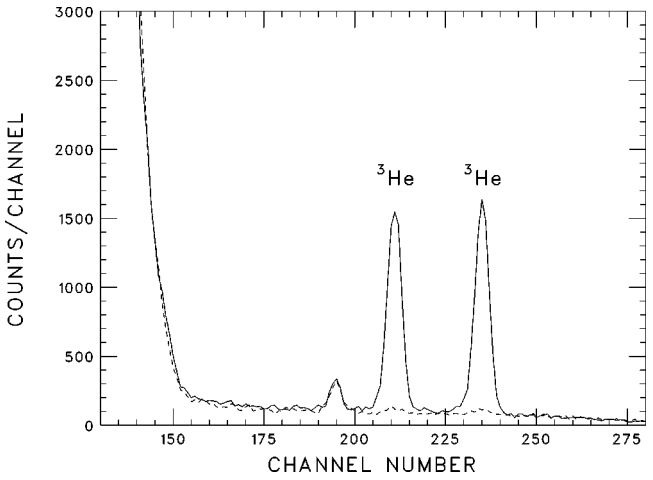

FIG. 3. Typical energy spectrum of ^{3}He recoils in a strip of the Si detector with (solid curve) and without (dashed curve) hydrogen gas in the target cell.

The ^{3}He counts were obtained for each peak by integrating the counts within the range nearly equal to FWHM. The width of the integration range was kept common for all the measurements with different magnetic substates of the $\vec{d}$ beam. From the ^{3}He counts in each strip for different $\vec{d}$ beam polarizations, the raw data for the analyzing powers of the pd capture were derived.

The raw data for A_{xx}, A_{yy}, and A_y^d were then corrected for the finite azimuthal angular range of the measurement. From the experimental geometry and the vertical angular spread of ^{3}He recoils in the previous subsection, the width of azimuthal angular spread was estimated to vary from $\pm 9°$ to $\pm 24°$, depending on the reaction angle $\theta_{c.m.}(^3He)$. The corrections were within 0.0008 for A_y^d, and within 0.0009 for A_{xx} and A_{yy}.

In the angular range of $67° \leqslant \theta_{c.m.} \leqslant 115°$ where ^{3}He particles were measured both on the left- and right-hand sides of the beam, the data were averaged to obtain the final results.

III. RESULTS AND COMPARISON WITH CALCULATIONS

Since $A_{xx}(\theta)$, $A_{yy}(\theta)$, and $A_{zz}(\theta)$ were measured separately by changing the beam polarization axis, the experimental data were examined if they satisfy the identity relation of $A_{xx}(\theta)+A_{yy}(\theta)+A_{zz}(\theta)=0$. Figure 4 shows the sum of the three analyzing powers as a function of reaction angle. The experimental data were found to fulfill the relation within 2.2 standard deviations. The average of the summed analyzing powers was 0.0011 ± 0.0013.

The individual analyzing powers are presented in Figs. 5–8, with error bars including the statistical ones and the ambiguities in the background subtraction. The uncertainty in the scale of the data is approximately 2%.

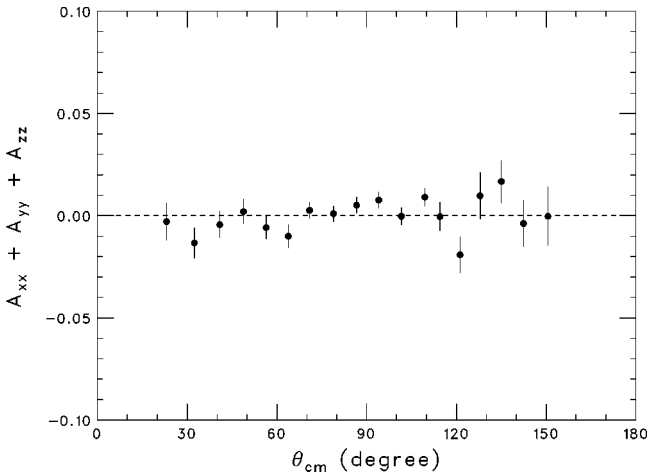

FIG. 4. Experimental examination of the identity relation of $A_{xx}(\theta)+A_{yy}(\theta)+A_{zz}(\theta)=0$.

Recently a Faddeev calculation of pd radiative capture was performed explicitly taking into account effects of meson exchange currents (MEC) in the electromagnetic interaction for the cases with and without including the Tucson-Melbourne type $\pi\pi 3NF$ [17]. Figures 5–8 also show the results of the calculation based on the AV_{18} $2NF$.

It is seen in that calculation that the $3NF$ effects are quite large in the tensor analyzing powers, which is contrary to the case of vector analyzing power. The calculation with the $\pi\pi 3NF$ is seen to well reproduce the present data for A_{xx} and A_y^d (see Figs. 5 and 7), whereas it underestimates the magnitudes of A_{yy} and A_{zz} (Figs. 6 and 7). These observations may suggest that accurate data set of tensor analyzing powers is of crucial importance in examining the effects of $3NF$. To extract the $3NF$ information from the present data, however, further calculations based on different $2NF$ potentials coupled with $3NF$ are necessary. Also the estimation of effects of Coulomb force is of importance.

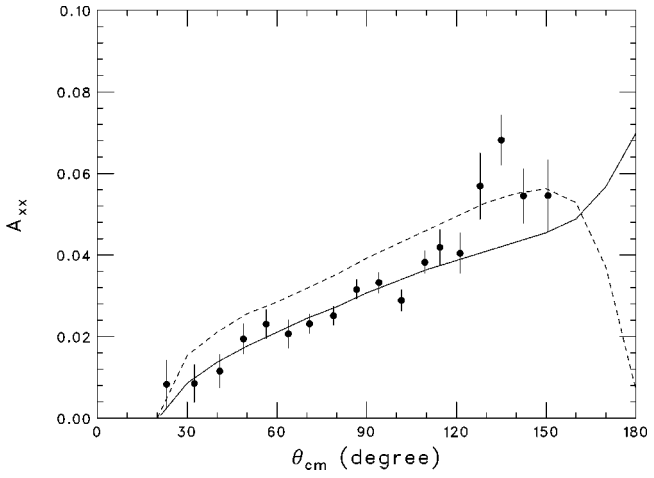

FIG. 5. A_{xx} of H($\vec{d}$,^{3}He)γ reaction at $E_d=17.5$ MeV. The error bars include the statistical error and small systematic uncertainty in the background subtraction. Curves are Faddeev calculations based on AV_{18} two-body potential with (solid line) and without (dashed line) the Tucson-Melbourne type $\pi\pi 3NF$ [17]. In the calculations meson exchange currents (MEC) are taken into account.

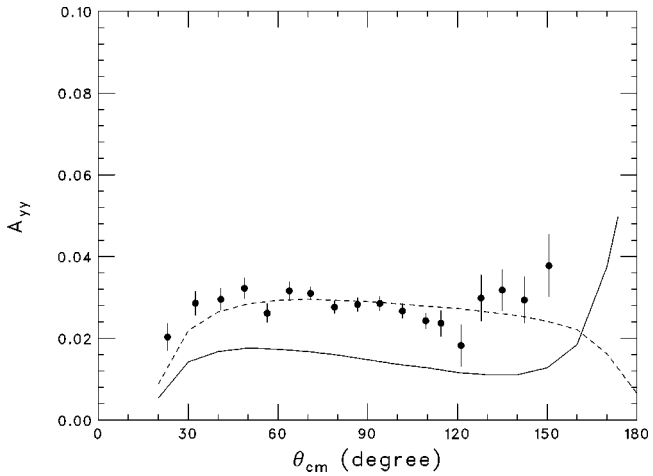

FIG. 6. A_{yy} of H($\vec{d}$,^{3}He)γ reaction at $E_d=17.5$ MeV. The error bars include the statistical error and small systematic uncertainty in the background subtraction. Curves are the same as presented in the captions to Fig. 5.

It is of value to examine here the energy dependence of the tensor analyzing powers by combining the present data and the previous ones obtained at several energies below 45 MeV. Since some of the previous data have only been obtained at $\theta_{lab}(\gamma)=90°$, the examination of the energy dependence is limited to the γ-ray laboratory angle of 90°. The angle corresponds to $\theta_{c.m.}(^3\mathrm{He})=85°$ in the present data, and the analyzing powers at this angle were obtained by assuming linear angular dependence in the range of $60° \leqslant \theta_{c.m.} \leqslant 119°$. The derived results at $\theta_{c.m.}(^3\mathrm{He})=85°$ are listed below. Also presented in the parentheses are the values at $\theta_{c.m.}(^3\mathrm{He})=90°$ derived in a similar manner for reference. The errors include the interpolation ambiguities and the scale uncertainties

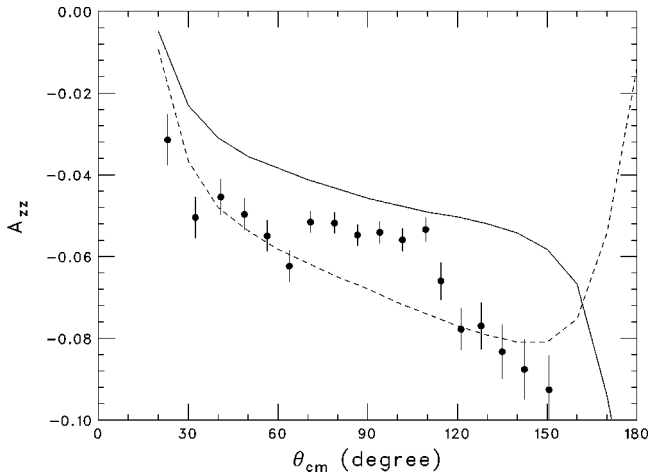

FIG. 7. A_{zz} of H($\vec{d}$,^{3}He)γ reaction at $E_d=17.5$ MeV. The error bars include the statistical error and small systematic uncertainty in the background subtraction. Curves are the same as presented in the captions to Fig. 5.

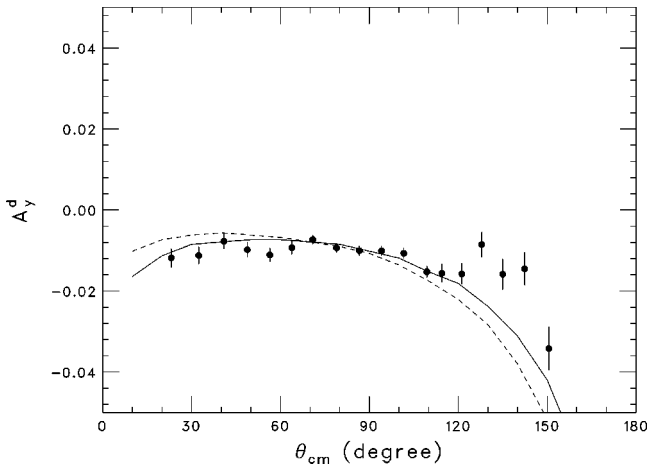

FIG. 8. A_y^d of H($\vec{d}$,^{3}He)γ reaction at $E_d=17.5$ MeV. The error bars include the statistical error and small systematic uncertainty in the background subtraction. Curves are the same as presented in the captions to Fig. 5.

$$A_{xx}=0.0283\pm0.0011 \quad (0.0301\pm0.0011),$$

$$A_{yy}=0.0285\pm0.0009 \quad (0.0277\pm0.0008),$$

$$A_{zz}=-0.0546\pm0.0015 \quad (-0.0549\pm0.0015).$$

The analyzing powers at $\theta_{\rm lab}(\gamma)=90°$ below 45 MeV are shown in Figs. 9 and 10. Energy dependence of A_{yy} is fairly well reproduced by the calculations based on the AV_{18} $2NF$ including the MEC effects but not including the $\pi\pi 3NF$ [17]. Further accumulation of accurate data is necessary for A_{zz}. Calculations of energy dependence of the analyzing powers based on various $2NF$ potentials with and without $\pi\pi 3NF$ are highly desired.

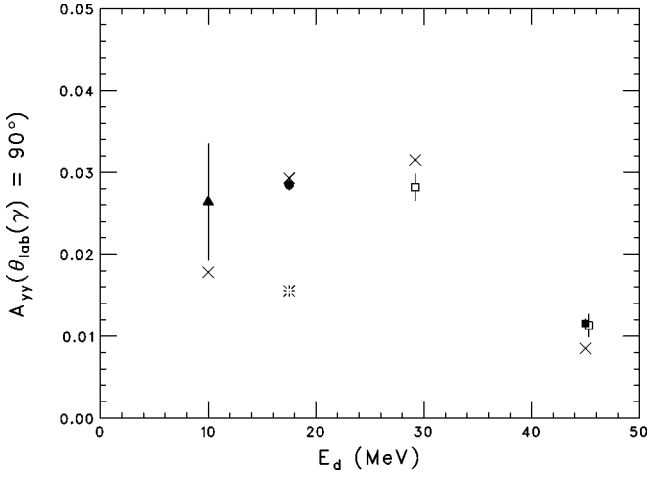

FIG. 9. $A_{yy}[\,\theta_{\rm lab}(\gamma)=90°\,]$ of H($\vec{d},\gamma$)^{3}He reaction. Experimental data are from Refs. [18] (solid triangle), [12] (open square), [13] (solid square), and the present study (solid circle). Faddeev calculations taking MEC into account in connection with AV_{18} $2NF$ with (asterisk) and without (cross) $\pi\pi 3NF$ [17] are also shown.

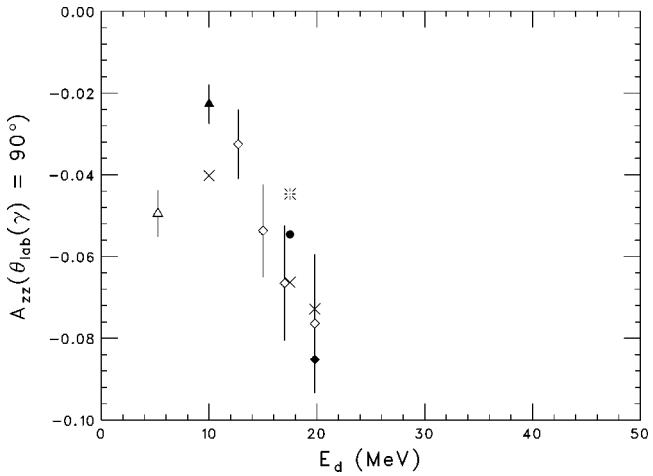

FIG. 10. $A_{zz}[\,\theta_{\rm lab}(\gamma)=90°\,]$ of H($\vec{d},\gamma$)^{3}He reaction. Experimental data are from Refs. [19] (open triangle), [18] (solid triangle), [20] (open diamond), [15] (solid diamond), and the present study (solid circle). Faddeev calculations taking MEC into account in connection with AV_{18} $2NF$ with (asterisk) and without (cross) $\pi\pi 3NF$ [17] are also shown.

IV. SUMMARY AND CONCLUSION

Angular distribution of analyzing powers $A_{xx}(\theta)$, $A_{yy}(\theta)$, $A_{zz}(\theta)$, and $A_y^d(\theta)$ of the H($\vec{d}$,^{3}He)γ reaction have been accurately measured at $E_d=17.5$ MeV. The use of a hydrogen gas target sealed with thin carbon foils were effective in observing ^{3}He recoils with enough statistics. The detection of ^{3}He recoils allowed achievement of high detection efficiency as well as measurement of angular distribution in a wide angular range. The experimental data satisfied the identity relation of $A_{xx}(\theta)+A_{yy}(\theta)+A_{zz}(\theta)=0$ virtually within statistical errors.

The recent Faddeev calculation [17] which takes MEC and $\pi\pi 3NF$ into account was found to reproduce $A_y^d(\theta)$ and $A_{xx}(\theta)$, while it underestimates the magnitudes of $A_{yy}(\theta)$ and $A_{zz}(\theta)$. The large effects of the $\pi\pi 3NF$ on the tensor analyzing powers, as predicted by the calculation, may imply the possibility of extracting the role of $\pi\pi 3NF$ from the tensor analyzing powers.

On the other hand, Golak and Witała [21] have shown from their pd capture calculation without $3NF$ that the charge-dependent modification of P-wave $2NF$, which is very effective in improving A_y prediction for Nd scattering [22], little affects analyzing powers of the pd capture below $E_d=45$ MeV. This may also indicate that the effect of $3NF$ may be investigated in the pd capture without interference with the problem of the P-wave $2NF$.

Further theoretical studies of the $3NF$ effect in the pd capture with various $2NF$'s are essential. The effect of Coulomb force neglected thus far should also be examined.

At energies higher than $E_d=130$ MeV, as indicated in the case of Nd scattering [4], the effect of $\pi\pi 3NF$ is expected to become relatively important in the pd radiative capture reaction. The effect of Coulomb force would become less important. A trial to measure several types of polarization observables at $E_d=200$ MeV is presently in progress.

ACKNOWLEDGMENTS

The authors would like to express their sincere appreciation to S. Ishikawa and H. Kamada for their useful communications and discussions, to S. Morinobu for his informative suggestions throughout the study, and to H. Koga and T. Maeda for their support in preparing apparatuses and electronic circuits. The support and help of A. Motoshima, R. Koyasako, and K. Nakashima during the experiment are gratefully acknowledged.

[1] T. Sasakawa, S. Ishikawa, Y. Wu, and T-Y. Saito, Phys. Rev. Lett. **68**, 3503 (1992).
[2] K. Sagara, H. Oguri, S. Shimizu, K. Maeda, H. Nakamura, T. Nakashima, and S. Morinobu, Phys. Rev. C **50**, 576 (1994).
[3] Y. Koike and S. Ishikawa, Nucl. Phys. **A631**, 683c (1998).
[4] H. Witała, W. Glöckle, D. Hüber, J. Golak, and H. Kamada, Phys. Rev. Lett. **81**, 1183 (1998).
[5] A. Kievsky, S. Rosati, W. Tornow, and M. Viviani, Nucl. Phys. **A607**, 402 (1996).
[6] J. Strate, K. Geissdorfer, R. Lin, W. Bielmeier, J. Cub, A. Ebneth, E. Finckh, H. Friess, G. Fuchs, K. Gebhardt, and S. Schindler, Nucl. Phys. **A501**, 51 (1989).
[7] G. Rauprich, S. Lemaitre, P. Niessen, K.R. Nyga, R. Reckenfelderbaumer, L. Sydow, H. Paetz gen Schieck, H. Witała, and W. Glöckle, Nucl. Phys. **A535**, 313 (1991).
[8] C.R. Howell, H.R. Setze, W. Tornow, R.T. Braun, W. Glöckle, A.H. Hussein, J.M. Lambert, G. Mertens, C.D. Roper, F. Salinas, I. Šlaus, D.E. González Trotter, B. Vlahović, R.L. Walter, and H. Witała, Nucl. Phys. **A631**, 692c (1998).
[9] E.O. Alt, A.M. Mukhamedzhanov, and A.I. Sattarov, Nucl. Phys. **A684**, 542c (2001).
[10] L.M. Qin, W. Boeglin, D. Fritschi, J. Götz, J. Jourdan, G. Masson, S. Robinson, I. Sick, P. Trueb, M. Tuccillo, B. Zihlmann, H. Witała, J. Golak, W. Glöckle, and D. Hüber, Nucl. Phys. **A587**, 252 (1995).
[11] S. Ishikawa and T. Sasakawa, Phys. Rev. C **45**, R1428 (1992).
[12] J. Jourdan, M. Baumgartner, S. Burzynski, P. Egelhof, R. Henneck, A. Klein, M.A. Pickar, G.R. Plattner, W.D. Ramsay, H.W. Roser, I. Sick, and J. Torre, Nucl. Phys. **A453**, 220 (1986).
[13] H. Anklin, L.J. de Bever, S. Buttazzoni, W. Glöckle, J. Golak, A. Honegger, J. Jourdan, H. Kamada, G. Kubon, T. Petitjean, L.M. Qin, I. Sick, Ph. Steiner, H. Witała, M. Zeier, J. Zhao, and B. Zihlmann, Nucl. Phys. **A636**, 189 (1998).
[14] M.C. Vetterli, J.A. Kuehner, C. Bamber, N. Davis, A.J. Trudel, H.R. Weller, and R.M. Whitton, Phys. Rev. C **38**, 2503 (1988).
[15] M.C. Vetterli, J.A. Kuehner, A.J. Trudel, C.L. Woods, R. Dymarz, A.A. Pilt, and H.R. Weller, Phys. Rev. Lett. **54**, 1129 (1985).
[16] S. Morinobu, computer code ORBIT2, 1987 (unpublished).
[17] J. Golak, K. Kamada, H. Witała, W. Glöckle, J. Kuroś-Zołnierczuk, R. Skibiński, V.V. Kotlyar, K. Sagara, and H. Akiyoshi, Phys. Rev. C **62**, 054005 (2000).
[18] F. Goeckner, W.K. Pitts, and L.D. Knutson, Phys. Rev. C **45**, R2536 (1992).
[19] K.P. Browne, W.K. Pitts, M.K. Smith, J.E. McAninch, and L.D. Knutson, Phys. Rev. C **54**, 1538 (1996).
[20] G.J. Schmid, R.M. Chasteler, H.R. Weller, D.R. Tilley, A.C. Fonseca, and D.R. Lehman, Phys. Rev. C **53**, 35 (1996).
[21] J. Golak and H. Witała, Few-Body Syst. **28**, 231 (2000).
[22] H. Witała and W. Glöckle, Nucl. Phys. **A528**, 48 (1991).